

# Femtosecond-pulse-driven, electron-excited XUV lasers in eight-times-ionized noble gases

B. E. Lemoff, C. P. J. Barty, and S. E. Harris

Edward L. Ginzton Laboratory, Stanford University, Stanford, California 94305

Received November 22, 1993

We propose three XUV laser schemes in the 30–50-nm wavelength region that can be driven by 10-Hz ultrashort-pulse terawatt laser systems. Tunneling ionization by circularly polarized radiation produces both the ions and hot electrons necessary to excite the upper laser level.

Electron excitation has been the mechanism of choice for the pumping of a wide variety of XUV lasers.<sup>1–3</sup> Recently Burnett and Corkum suggested using high-intensity ultrashort optical pulses to pump both recombination lasers<sup>4</sup> and electron-excited lasers.<sup>5</sup> In the latter method, intense circularly polarized light is used to create both the highly ionized species and the hot pumping electrons. In this Letter we model three specific systems of this type: Ar IX (Ne-like), lasing at 48 nm; Kr IX (Ni-like), lasing at 32 nm; and Xe IX (Pd-like), lasing at 41 nm. Our calculations indicate that each of these systems should produce high XUV gain. These systems are longitudinally pumped, consisting of  $\leq 1$  Torr of Ar, Kr, or Xe in a differentially pumped cell, into which a circular polarized femtosecond laser pulse is focused to an intensity of between  $10^{16}$  and  $10^{17}$  W/cm<sup>2</sup>. Tunneling ionization fully strips the outer shell and produces electrons with sufficient energy to excite collisionally the upper laser level.

Figure 1 shows the energy-level diagrams for the three laser systems. The atomic energy levels and dipole matrix elements were calculated with the RCN/RCG Atomic Physics Code of Cowan<sup>6</sup> and have an uncertainty of less than 10%. Transitions from the predominantly singlet states shown in Fig. 1 to predominantly triplet states have been included in all the calculations but have been omitted from the figure for the sake of simplicity. As with the Ne-like and Ni-like x-ray lasers first studied at Lawrence Livermore National Laboratory,<sup>1,2</sup> these systems are pumped by monopole electron excitation from ground.

Because the ionizing femtosecond laser pulses are much shorter than any multiparticle interaction times, we approximate the ionization rates and resulting electron energy distributions by those calculated for isolated atoms. Because we are using circularly polarized light, the instantaneous ionization rate may be computed by the tunneling formula for a static electric field, as given in Eq. (3) of Ref. 4. As an example of the thresholdlike behavior of tunneling ionization, consider the ionization of Ar VIII. Laser intensities of  $4.3 \times 10^{16}$ ,  $5.3 \times 10^{16}$ , and  $6.6 \times 10^{16}$  W/cm<sup>2</sup> result in ionization rates of  $10^{13}$ ,  $10^{14}$ , and  $10^{15}$  s<sup>-1</sup>, respectively. Figure 2 shows the laser intensity required for ionization of our species of interest in a time of 10 fs. The threshold intensity

required for ionization of the ninth electron is a factor of 7, 9, and 48 times higher than that required to ionize the eighth electron in Xe, Kr, and Ar, respectively. Thus, over a sizable portion of the beam profile, we expect the plasmas to consist entirely of eight-times-ionized species.

Theory also predicts that electrons produced by tunneling ionization with circularly polarized light will retain a kinetic energy equal to the quiver energy,  $\varepsilon = e^2 E^2 / 4m\omega^2$ , after the pulse has finished, where  $E$  is the instantaneous electric-field strength at the time of ionization.<sup>5</sup> With this assumption for electron energy, and assuming the ionization rate to be given by the static tunneling formula, the electron energy distribution can be numerically calculated for any laser pulse. For laser pulses whose peak intensity is great enough to fully strip the outer shell of our noble gases, we expect an initial electron energy distribution consisting of eight equal populations of electrons, each peaked about the quiver energy required for ionization of the corresponding ionization stage. Figure 3 shows the initial electron energy distribution calculated for Ar when it is subjected to a 30-fs Gaussian pulse with a peak intensity of  $10^{17}$  W/cm<sup>2</sup>. For the purpose of computing electron-induced transi-

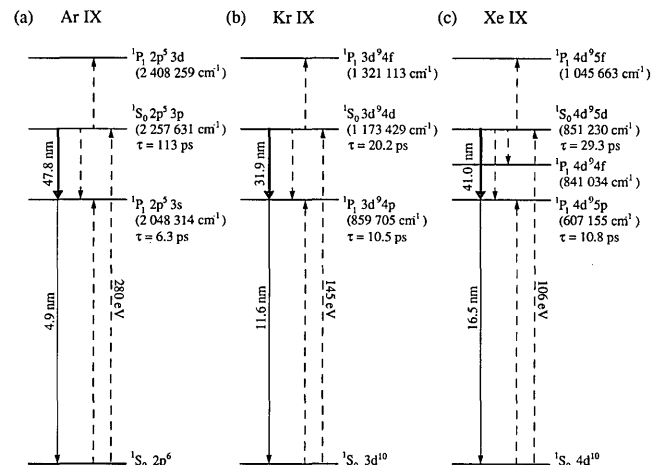


Fig. 1. Energy-level diagram of (a) Ar IX, (b) Kr IX, and (c) Xe IX lasers. The dashed lines indicate the most significant electron-induced transitions, and the solid lines indicate radiative transitions.

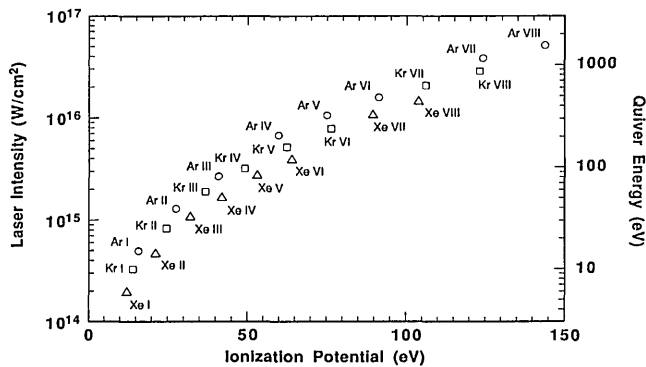


Fig. 2. Circularly polarized laser intensity required for production of an ionization rate of  $10^{14} \text{ s}^{-1}$  in the indicated species. Also shown is the corresponding quiver energy at 800 nm.

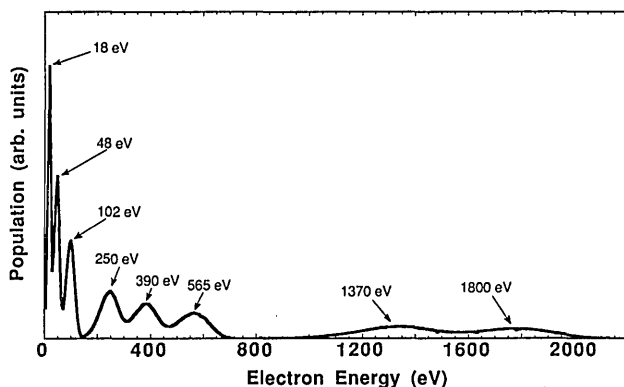


Fig. 3. Calculated initial electron energy distribution produced in Ar by a circularly polarized 30-fs FWHM Gaussian pulse of peak intensity  $10^{17} \text{ W/cm}^2$ .

tion rates, we approximate this distribution by eight delta functions in energy, ranging from 18 to 1800 eV in Ar, 12 to 1050 eV in Kr, and 9 to 550 eV in Xe. Assuming that the initial gas is at room temperature (0.025 eV), we use conservation of momentum to estimate our initial ion temperatures to be 0.087, 0.052, and 0.031 eV in Ar IX, Kr IX, and Xe IX, respectively. For the densities that we are considering, the time evolution of the electron and ion energy distributions is dominated by elastic collisions and can be estimated by the equations of Spitzer<sup>7</sup> and a simple numerical routine.

For determination of the inversion density in our laser systems, it is necessary to calculate the excitation rates of the upper and lower laser levels and the depopulation rate of the upper laser level. The Cowan Code calculates modified Born collision cross sections that are accurate to better than 50%, even at threshold, where the normal Born approximation breaks down.<sup>6</sup> For each transition, summing the calculated rate per unit electron density over those electron classes that are above threshold yields the transition rate per unit ion density. Table 1 lists these rates for the most important transitions. Assuming the lower laser level to be trapped, and the electron energy distribution to be constant over the lifetime of the upper level (an assumption supported

by our analysis), we estimate the maximum inversion density by

$$N_{\text{max}}^* = N_i^2 \left( R_{\text{upper}} - \frac{1}{3} R_{\text{lower}} \right) \left( \frac{1}{\tau_{\text{upper}}} + N_i R_{\text{out}} \right)^{-1}, \quad (1)$$

where  $N_i$  is the ion density;  $R_{\text{upper}}$ ,  $R_{\text{lower}}$ , and  $R_{\text{out}}$  are the electron-induced rates per unit ion density into the upper, into the lower, and out of the upper laser levels, respectively; and  $\tau_{\text{upper}}$  is the radiative lifetime of the upper level. It should be pointed out that the pump rate is rather insensitive to the precise electron energy distribution. For an electron whose energy is above the pumping threshold, a tenfold increase in electron energy will decrease the excitation rate by only a factor of approximately 2.

To compute the stimulated emission cross section, we assume a Lorentzian line shape with a full width equal to the quadrature sum of the homogeneous linewidth, the Doppler linewidth, and the electron-induced Stark linewidth. The increase in the homogeneous linewidth resulting from electron-collisional depopulation can be quickly calculated from the rates given in Table 1. We estimate the Stark linewidths by using the modified semiempirical method of Dimitrijevic and Konjevic<sup>8</sup> in the high-temperature limit, with the atomic dipole matrix elements calculated by the Cowan Code. We believe the uncertainty of these estimates to be less than a factor of 2. We calculate the spontaneous decay rate of the upper laser level into a single state of the lower level to be 2.0, 13.7, and  $10.2 \text{ ns}^{-1}$  in Ar, Kr, and Xe, respectively. Table 2 summarizes our calculations for the Ar, Kr, and Xe systems, each at two different densities.

For the systems listed in Table 2 to achieve a gain-length product of 20, lengths ranging from 2 to 27 mm will be necessary. Thus the driving laser must be focused to a sufficient intensity to produce eight-times-ionized species over these lengths. For the Xe system at  $10^{17}/\text{cm}^3$ , focusing to an intensity

Table 1. Electron-Induced Transition Rates Per Unit Ion Density<sup>a</sup>

Ion	Transition	$R \text{ (cm}^3/\text{s)}$
Ar IX	$^1S_0 2p^6 \rightarrow ^1P_1 2p^5 3s$	$2.3 \times 10^{-10}$
	$^1S_0 2p^6 \rightarrow ^1S_0 2p^5 3p$	$1.6 \times 10^{-9}$
	$^1S_0 2p^5 3p \rightarrow ^1P_1 2p^5 3s$	$5.9 \times 10^{-8}$
	$^1S_0 2p^5 3p \rightarrow ^1P_1 2p^5 3d$	$1.1 \times 10^{-7}$
Kr IX	$^1S_0 3d^{10} \rightarrow ^1P_1 3d^9 4p$	$7.3 \times 10^{-9}$
	$^1S_0 3d^{10} \rightarrow ^1S_0 3d^9 4d$	$9.9 \times 10^{-9}$
	$^1S_0 3d^9 4d \rightarrow ^1P_1 3d^9 4p$	$7.9 \times 10^{-8}$
	$^1S_0 3d^9 4d \rightarrow ^1P_1 3d^9 4f$	$1.9 \times 10^{-7}$
Xe IX	$^1S_0 4d^{10} \rightarrow ^1P_1 4d^9 5p$	$1.3 \times 10^{-8}$
	$^1S_0 4d^{10} \rightarrow ^1S_0 4d^9 5d$	$1.5 \times 10^{-8}$
	$^1S_0 4d^9 5d \rightarrow ^1P_1 4d^9 5p$	$1.7 \times 10^{-7}$
	$^1S_0 4d^9 5d \rightarrow ^1P_1 4d^9 4f$	$3.2 \times 10^{-7}$
	$^1S_0 4d^9 5d \rightarrow ^1P_1 4d^9 5f$	$1.7 \times 10^{-7}$

<sup>a</sup>Rates given are already summed over degenerate states.

**Table 2. Predicted Homogeneous Linewidth Including Electron Collisions ( $\Gamma_H$ ), Doppler Width ( $\Gamma_D$ ), Stark Width ( $\Gamma_S$ ), Maximum Inversion Density ( $N_{\max}^*$ ), and Gain of Ar IX, Kr IX, and Xe IX Laser Lines**

Laser Line	Density ( $\text{cm}^{-3}$ )	$\Gamma_H$ ( $\text{ns}^{-1}$ )	$\Gamma_D$ ( $\text{ns}^{-1}$ )	$\Gamma_S$ ( $\text{ns}^{-1}$ )	$N_{\max}^*$ ( $\text{cm}^{-3}$ )	Gain ( $\text{cm}^{-1}$ )
Ar IX	$2 \times 10^{17}$	165	143	170	$1.3 \times 10^{15}$	34
47.8 nm	$1 \times 10^{17}$	161	143	85.4	$5.5 \times 10^{14}$	17
Kr IX	$1 \times 10^{17}$	122	115	164	$1.0 \times 10^{15}$	94
31.9 nm	$2 \times 10^{16}$	110	115	32.8	$5.5 \times 10^{13}$	7.5
Xe IX	$1 \times 10^{17}$	136	56	240	$1.1 \times 10^{15}$	107
41.0 nm	$2 \times 10^{16}$	104	56	48	$9.0 \times 10^{13}$	20

of  $\geq 1.5 \times 10^{16}$  W/cm<sup>2</sup> over a length of 2 mm would require a diffraction-limited 0.1-TW laser pulse, whereas for the Ar system at  $10^{17}$ /cm<sup>3</sup>, focusing to an intensity of  $\geq 5.2 \times 10^{16}$  W/cm<sup>2</sup> over a length of 12 mm would require a diffraction-limited 2.6-TW laser pulse.

To avoid termination of lasing due to trapping, one must make sure that the lower-level decay photon has an absorption length longer than the radius of the laser volume. At the calculated initial ion temperature and ion density of  $10^{17}$ /cm<sup>3</sup>, a 4.9-nm photon in Ar IX, an 11.6-nm photon in Kr IX, and a 16.4-nm photon in Xe IX have absorption lengths of 15.7, 1.1, and 0.23  $\mu\text{m}$ , respectively. An ideal 800-nm beam with a confocal parameter of 1 cm has a waist of  $\sim 36$   $\mu\text{m}$ . Thus in such a geometry all three systems should terminate after one or two lifetimes of the upper level. As the ions heat, these absorption lengths increase as a result of increased Doppler width. Our time evolution analysis indicates that the heavy Kr IX and Xe IX ions never heat enough to avoid trapping. The lighter Ar IX ions reach a temperature, after several hundred picoseconds, that is high enough to permit the lower laser level to empty. In addition, electron thermalization will have resulted in all electrons' being above the pumping threshold by this time. Thus we predict that the Ar IX system can lase continuously for several nanoseconds until inelastic electron cooling causes lasing to terminate.

Pump beam defocusing puts limits on the length and density of the system. In cases in which the electron density is proportional to the laser beam intensity profile, an optical phase shift of  $\pi$  rad at beam center is often considered to be the point at which self-defocusing becomes significant. For an 800-nm laser, an electron-density-length product of  $1.4 \times 10^{17}$ /cm<sup>2</sup> will produce an optical phase delay of  $\pi$  rad. In our experiment, once the laser exceeds a threshold intensity all ions are eight times ionized. Thus the electron density and index of refraction should be uniform over a sizable region of the beam profile once the leading edge of the pulse has passed. Furthermore, the steplike behavior of tunneling ionization means that the dominant beam defocusing effects will be at the interfaces between regions that are entirely  $n$  times ionized and regions that are entirely  $n - 1$  time ionized. Thus we expect that, in a

differentially pumped system, in which the beam encounters matter only within its confocal parameter, lengths in excess of 1 cm should be achievable at an ion density of  $10^{17}$ /cm<sup>3</sup>.

In conclusion, we have proposed three specific electron-excited XUV laser schemes that can be driven with short-pulse terawatt laser systems. The use of circular polarization is required for energetic electrons to be produced. These systems require rather low densities and can be end pumped over lengths exceeding 1 cm. The predicted gains are sufficiently high that we expect to see saturated output, even over lengths of only a few millimeters.

The authors thank S. J. Benerofe and J. E. Field for their assistance. This research was supported by the U.S. Air Force Office of Scientific Research, the U.S. Army Research Office, and the Strategic Defense Initiative Organization.

## References

1. D. L. Matthews, P. L. Hagelstein, M. D. Rosen, M. J. Eckart, N. M. Ceglio, A. U. Hazi, B. J. MacGowan, J. E. Trebes, B. L. Whitten, E. M. Campbell, C. W. Hatcher, A. M. Hawryluk, R. L. Kauffman, L. D. Pleasance, G. Rambach, J. H. Scofield, G. Stone, and T. A. Weaver, *Phys. Rev. Lett.* **54**, 110 (1985).
2. B. J. MacGowan, S. Maxon, C. J. Keane, R. A. London, D. L. Matthews, and D. A. Whelan, *J. Opt. Soc. Am. B* **5**, 1858 (1988).
3. C. P. J. Barty, D. A. King, G. Y. Yin, K. H. Hahn, J. E. Field, J. F. Young, and S. E. Harris, *Phys. Rev. Lett.* **61**, 2201 (1988).
4. N. H. Burnett and P. B. Corkum, *J. Opt. Soc. Am. B* **6**, 1195 (1989).
5. P. B. Corkum and N. H. Burnett, in *Short-Wavelength Coherent Radiation: Generation and Applications*, R. W. Falcone and J. Kirz, eds., Vol. 2 of OSA Proceedings Series (Optical Society of America, Washington, D.C., 1988), p. 225.
6. R. D. Cowan, *The Theory of Atomic Structure and Spectra* (U. of Calif. Press, Berkeley, Calif., 1981), Secs. 8-1, 16-1, and 18-13.
7. L. Spitzer, *Physics of Fully Ionized Gases* (Interscience, London, 1962), Sec. 5.3.
8. M. S. Dimitrijevic and N. Konjevic, in *Spectral Line Shapes*, B. Wende, ed. (de Gruyter, Berlin, 1981), p. 211.